

Nuclear profile dependence of elliptic flow from a parton cascade

Bin Zhang

*Department of Chemistry and Physics, Arkansas State University,
P.O. Box 419, State University, Arkansas 72467-0419, USA*

Abstract

The transverse profile dependence of elliptic flow is studied in a parton cascade model. We compare results from the binary scaling profile to results from the wounded nucleon scaling profile. The impact parameter dependence of elliptic flow is shown to depend sensitively on the transverse profile of initial particles, however, if elliptic flow is plotted as a function of the relative multiplicity, the nuclear profile dependence disappears. The insensitivity was found previously in a hydrodynamical calculation. Our calculations indicate that the insensitivity is also valid with additional viscous corrections. In addition, the minimum bias differential elliptic flow is demonstrated to be insensitive to the nuclear profile of the system.

Key words: elliptic flow, parton cascade, relativistic heavy ion collisions

PACS: 25.75.-q,25.75.Ld,24.10.Lx

Recently, the Relativistic Heavy Ion Collider has produced large amount of exciting new data. These new data give us valuable insight into the hot and dense nuclear matter. One of the important observables is elliptic flow which reflects the transverse anisotropy of particle momentum distribution. Elliptic

flow has been studied by many theoretical models, including non-Abelian energy loss models [1,2], saturation models [3,4,5], parton recombination models [6,7,8,9,10,11,12,13], hydrodynamical models [14,15,16], and parton cascade models [17,18,19]. In this paper, we will study the elliptic flow using a parton cascade model. We will first introduce the elliptic flow, and the parton cascade model used for this study. Then, we will use the parton cascade model to study the elliptic flow produced from two different initial transverse distributions, one proportional to the number of binary collisions, one proportional to the number of wounded nucleons. We demonstrate that even though, elliptic flow as a function of the impact parameter is very sensitive to the initial transverse distribution of particles, elliptic flow as a function of the relative multiplicity is almost independent of the transverse distribution. Furthermore, we show that the minimum bias differential elliptic flow is also insensitive to the initial transverse particle distribution.

Elliptic flow is the elliptic deformation in the particle transverse momentum distribution [20]. It is usually characterized by the second Fourier coefficient of the particle azimuthal distribution [21]. If we use $f(\phi)$ for the azimuthal distribution, and choose the azimuthal angle of the reaction plane to be zero, then

$$f(\phi) = v_0 + 2v_1 \cos(\phi) + 2v_2 \cos(2\phi) + \dots \quad (1)$$

The coefficient, v_2 , is the elliptic flow observable. It is the average of $\cos(2\phi)$ of produced particles. If the transverse components of the momenta are known, it can be calculated by:

$$v_2 = \left\langle \frac{p_x^2 - p_y^2}{p_x^2 + p_y^2} \right\rangle. \quad (2)$$

In the above formula, $\langle \dots \rangle$ denotes the average over particles. Since initial momentum distribution is isotropic, the elliptic flow is generated by final state interactions. Final state interactions (or pressure gradient) turn(s) the spatial anisotropy into momentum space anisotropy. It has been shown that the elliptic flow is very sensitive to the initial stage evolution, and can be used as a sensitive probe of early dynamics [22,23].

In the following, we are going to use Zhang's Parton Cascade (ZPC) [24] to study elliptic flow at relativistic energies. The initial conditions are set up similar to those in a recent study by Molnar's Parton Cascade (MPC) [18]. In the local rest frame, the initial momentum distribution is thermal, with a temperature of 700 MeV. Particles are uniformly distributed between a space time rapidity of -5 and +5. The particle formation proper time is 0.1 fm/c. There are totally 2100 gluons per central event. As the momentum transport is determined by the momentum opacity, the following results are also correct if the total number of particles increases and the transport cross section decreases by the same factor. To efficiently simulate momentum transport, we use isotropic differential cross sections that preserve the reaction plane of a collision. The total parton-parton elastic cross section σ_{gg} will be varied to have values of 40 mb, 20 mb, 10 mb to study the response of the system. These cross sections are effective cross sections as no radiative energy loss or parton recombinations are included in the calculations.

We will study the elliptic flow produced from two different initial transverse spatial distributions. One is proportional to the number of binary collisions per unit area. In this case, the particle number as a function of the impact parameter is also proportional to the number of binary collisions. The other distribution is proportional to the number of wounded nucleons per unit area

and the particle number as a function of the impact parameter is also proportional to the number of wounded nucleons. In generating the above distributions, the nucleon-nucleon inelastic cross section σ_{NN} is taken to be 40 mb, and the three parameter Woods-Saxon distribution is used for the nucleons inside one nucleus. These two spatial distributions are related to hard and soft particle production mechanisms, respectively [16].

The above initial spatial distribution and initial momentum distribution factorize. As local densities are sampled for the evolution of the expanding parton system according to the Boltzmann equation, the factorization is not automatically conserved. We also note that a geometry with sharp cylindrical nuclei always leads to larger elliptic flow values compared to the binary collision scaling case [1,17,18,25,26].

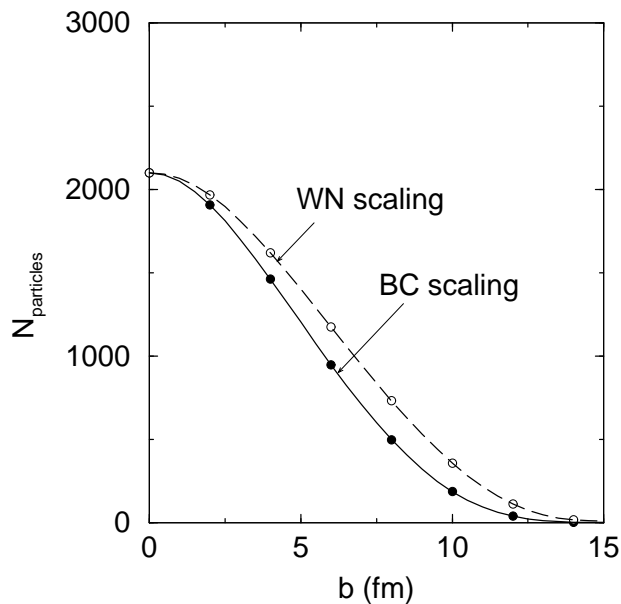


Fig. 1. Number of particles as a function of the impact parameter for the binary collision (BC) scaling case and the wounded nucleon (WN) scaling case. Circles are generated by the simulation code.

Fig. 1 gives the number of particles as a function of the impact parameter.

While the two distributions have the same number of particles when $b = 0$, the wounded nucleon scaling has more particles than the binary collision scaling case. In particular, when $b = 10$ fm, the wounded nucleon scaling has about twice as many particles as the binary collision scaling case. Fig. 2 has the initial spatial ellipticity as a function of the impact parameter. The initial spatial ellipticity in the figure is defined through

$$\epsilon = \left\langle \frac{y^2 - x^2}{y^2 + x^2} \right\rangle. \quad (3)$$

Note that this definition calculates the ratio first and then the average and the magnitude is smaller than the ratio of the averages.

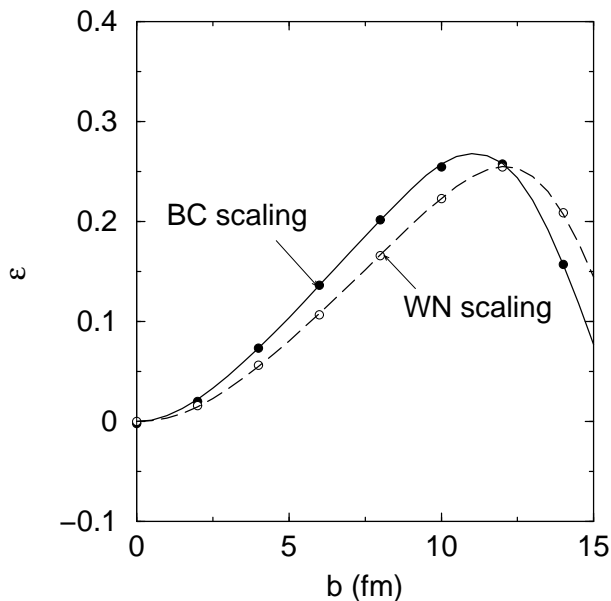


Fig. 2. Initial spatial ellipticity as a function of the impact parameter.

We first study the impact parameter dependence of the elliptic flow. The set up is similar to the recent MPC model study [18]. We approach the Boltzmann limit by increasing the number of particles and at the same time decreasing the cross section by the same factor [17,18,27,28]. In the binary collision scaling case, the rescaling factors for $b = 0, 2, 4, 6, 8, 10, 12, 14$ fm are

$\lambda = 100, 100, 100, 220, 450, 1100, 5000, 50000$. In the wounded nucleon scaling case, the rescaling factors are $\lambda = 100, 100, 100, 200, 300, 600, 2000, 11000$. The convergence is checked by comparing to calculations done with $\lambda/2$. The v_2 is calculated for particles with a rapidity range of $|y| < 2$.

From Fig. 3, we observe that as the total cross section increases, or more precisely, as the transport cross section increases, the elliptic flow increases. The binary collision scaling case is larger than the wounded nucleon scaling case for small impact parameters and smaller than the wounded nucleon scaling case for large impact parameters. This follows the trend of the initial spatial ellipticity. However, the v_2 curves peak at smaller impact parameters than the ϵ curves. This indicates that both initial ellipticity and initial particle density play roles in determining the elliptic flow. As the impact parameter increases, the elliptic flow increases with the initial ellipticity, however, after a point, the particle density is not high enough to generate enough response and the elliptic flow can not catch up with the initial ellipticity. It starts decreasing with increasing impact parameter.

An alternative way of characterizing centrality is to use the relative central rapidity density, which is the ratio of the central rapidity density to that in central collisions with $b = 0$. If we plot the elliptic flow as a function of the relative central rapidity density as in Fig. 4, we see that for the same transport cross section, the two curves corresponding to the binary collision scaling and the wounded nucleon scaling overlap. In other words, the impact parameter dependence of elliptic flow is cancelled by the impact parameter dependence of the multiplicity. Similar observations have been made in a recent hydrodynamics study [16]. This indicates that if we use the relative central rapidity density as a measure of centrality, the elliptic flow is not sensitive to whether

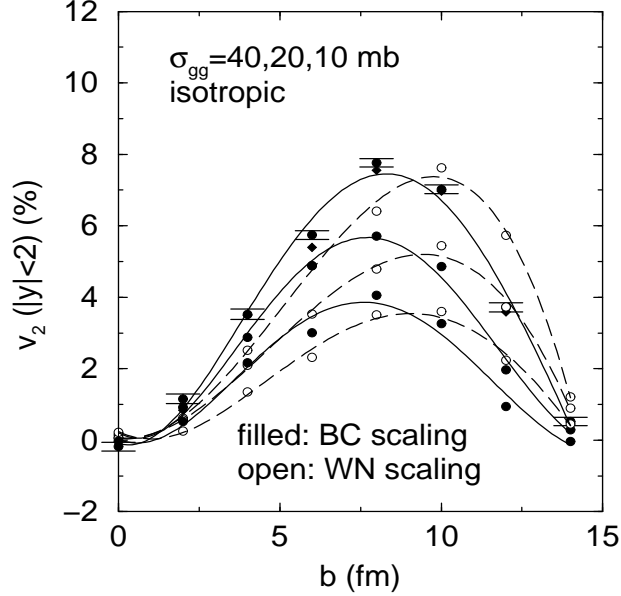


Fig. 3. Elliptic flow as a function of the impact parameter. Filled symbols are for the binary collision scaling case and open symbols are for the wounded nucleon scaling case. The curves are used to guide the eyes. Going from above, the three sets of results are for $\sigma_{gg} = 40, 20, 10$ mb, respectively. For the binary collision scaling with $\sigma_{gg} = 40$ mb case, the statistical error bars are also drawn. They are about the same for other curves. The diamonds are results for the binary collision case with $\sigma_{gg} = 40$ mb and parton number rescaling factor of $\lambda/2$. They agree well with the case with λ particle division.

the initial distribution is binary collision scaling or wounded nucleon scaling. It reflects the particle transport cross section, or in the case of hydrodynamics, the equation of state. Because of the viscous corrections, the cascade calculations have a bend over when the relative central rapidity density is small. In contrast, the hydrodynamic calculations have an almost straight line dependence and overshoot data when the relative rapidity density is small. We also note that the $\sigma_{gg} = 40$ mb binary collision scaling case is consistent with set D of [18].

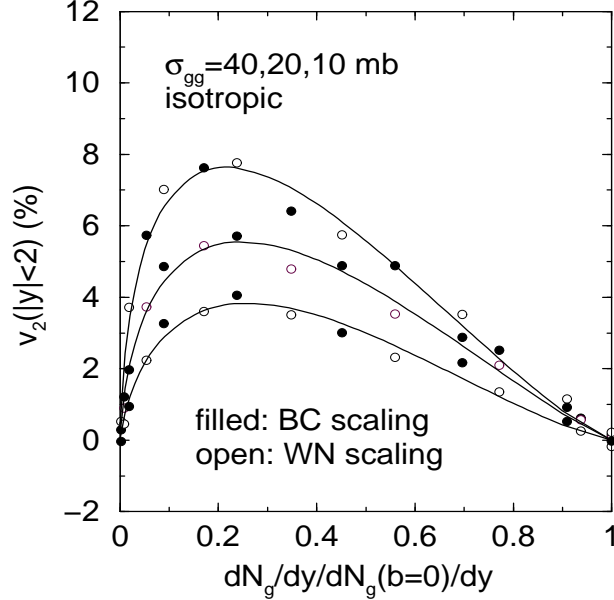


Fig. 4. Elliptic flow as a function of the relative rapidity density. Meanings of symbols are the same as those in Fig. 3.

Now we turn to the study of p_t differential elliptic flow which can give further information about the evolution [29]. Hydrodynamic studies agree well with low p_t data. At $p_t > 2$ GeV, the data are consistent with a constant behavior while hydrodynamic results keep on increasing. In dynamic models, only when viscous effects are taken into account, is it possible to describe the deviation from the ideal hydrodynamical behavior. A recent hydrodynamic study demonstrates that the minimum bias p_t differential flow is not sensitive to the initial nuclear profile. We want to know whether it is also true when viscous effects are taken into account. Fig. 5 shows the impact parameter averaged p_t differential flow. The calculations with binary collision scaling agree well with those with wounded nucleon scaling. This is true not only for the low p_t region, but also for the high p_t region where viscous effects are important.

Another way of averaging over events is to calculate the multiplicity weighted average of cosine of the azimuthal angle. This gives the minimum bias elliptic

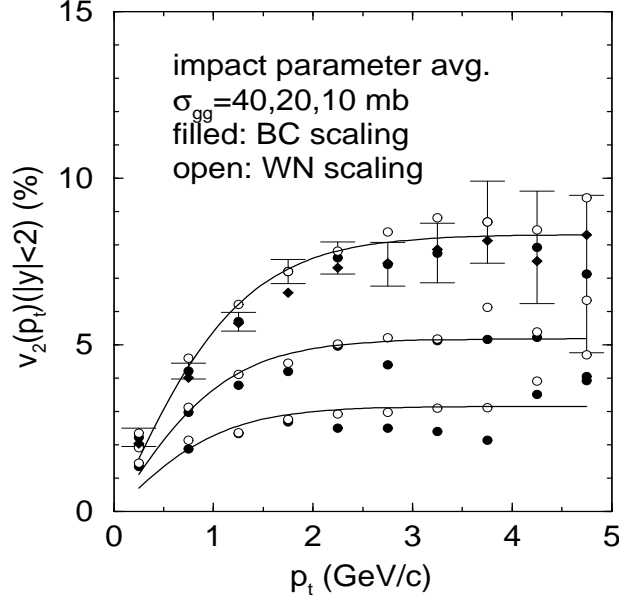


Fig. 5. Impact parameter averaged differential elliptic flow as a function of the transverse momentum. Meanings of symbols are the same as those in Fig. 3.

flow. Results from the ZPC model are shown in Fig. 6. The binary collision scaling and the wounded nucleon scaling agree well with each other. This further demonstrates that the minimum bias p_t differential elliptic flow is insensitive to the initial nuclear profile. A comparison of Fig. 5 and Fig. 6 shows that the minimum bias results are about 10% higher than the impact parameter averages. Hence the impact parameter averaged differential elliptic flow can be considered as a reasonably good approximation of the minimum bias differential elliptic flow. As pointed out in [18], the minimum bias elliptic flow weights in more central events. The central events in the wounded nucleon scaling case have lower elliptic flow than those in the binary collision scaling case. This can lead to a relatively smaller minimum bias elliptic flow in the wounded nucleon scaling case. However, the decrease in the relative amplitude can not be determined with the current statistics.

In summary, we demonstrate that the elliptic flow as a function of relative

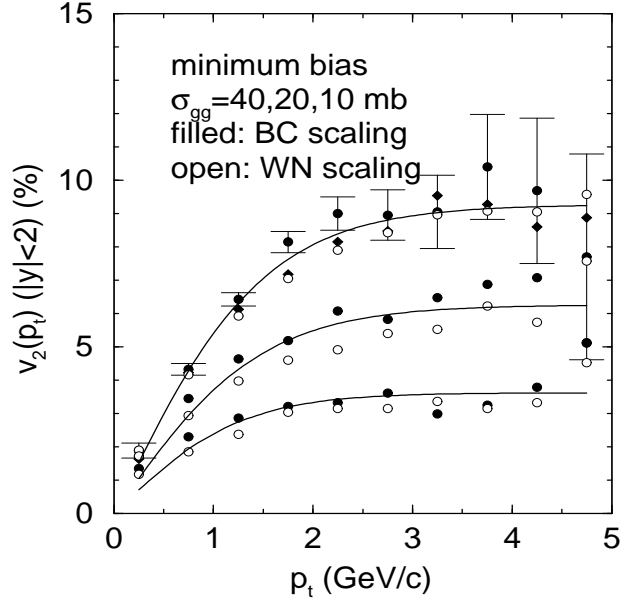


Fig. 6. Minimum bias differential elliptic flow as a function of the transverse momentum. Meanings of symbols are the same as those in Fig. 3.

central rapidity density in the binary scaling case agrees well with that in the wounded nucleon case. In addition, the minimum bias p_t differential elliptic flow in the binary scaling case also agrees well with that in the wounded nucleon case. This is true not only for the low p_t region, but also for the high p_t region where viscous effects are important and ideal hydrodynamics deviates from experimental data. As hadronization will not change the high p_t elliptic flow [18], and recent research indicates the possibility of extracting the parton elliptic flow from hadron elliptic flow [8], the elliptic flow as a function of relative rapidity density and the minimum bias p_t differential elliptic flow are promising observables for the extraction of information about final state interactions [30].

This work was supported by the U.S. National Science Foundation under Grant No. 0140046. We thank P. Kolb, Z.W. Lin, D. Molnar, and A. Poskanzer for helpful discussions. We also thank the Parallel Distributed System Facil-

ity at the National Energy Research Scientific Computer Center for providing computer resources.

References

- [1] M. Gyulassy, I. Vitev, X. N. Wang, Phys. Rev. Lett. 86 (2001) 2537.
- [2] M. Gyulassy, I. Vitev, X. N. Wang, P. Houvinen, Phys. Lett. B 526 (2002) 301.
- [3] A. Krasnitz, Y. Nara, R. Venugopalan, Nucl. Phys. A 702 (2002) 227.
- [4] D. Teaney, R. Venugopalan, Phys. Lett. B 539 (2002) 53.
- [5] Y. V. Kovchegov, K. L. Tuchin, Nucl. Phys. A 708 (2002) 413.
- [6] Z. W. Lin, C. M. Ko, Phys. Rev. Lett. 89 (2002) 202302.
- [7] D. Molnar, S. A. Voloshin, Phys. Rev. Lett. 91 (2003) 092301.
- [8] Z. W. Lin, D. Molnar, Phys. Rev. C 68 (2003) 044901.
- [9] R. J. Fries, B. Müller, C. Nonaka, S. A. Bass, Phys. Rev. Lett. 90 (2003) 202303.
- [10] V. Greco, C. M. Ko, P. Levai, nucl-th/0301093.
- [11] V. Greco, C. M. Ko, P. Levai, Phys. Rev. C 68 (2003) 034904.
- [12] R. J. Fries, B. Müller, C. Nonaka, S. A. Bass, nucl-th/0306027.
- [13] C. Nonaka, R. Fries, S. A. Bass, nucl-th/0308051.
- [14] D. Teaney, J. Lauret, E. V. Shuryak, Phys. Rev. Lett. 86 (2001) 4783.
- [15] P. F. Kolb, J. Sollfrank, U. W. Heinz, Phys. Rev. C 62 (2000) 054909.
- [16] P. F. Kolb, U. W. Heinz, P. Houvinen, K. J. Eskola, K. Tuominen, Nucl. Phys. A 696 (2001) 197.

- [17] B. Zhang, M. Gyulassy, C. M. Ko, Phys. Lett. B 455 (1999) 45.
- [18] D. Molnar, M. Gyulassy, Nucl. Phys. A 697 (2002) 495.
- [19] Z. W. Lin, C. M. Ko, Phys. Rev. C 65 (2002) 034904.
- [20] J. Ollitrault, Phys. Rev. D 46 (1992) 229.
- [21] S. Voloshin, Y. Zhang Z. Phys. C70 (1996) 665.
- [22] H. Sorge, Phys. Rev. Lett. 78 (1997) 2309.
- [23] H. Sorge, Phys. Rev. Lett. 82 (1999) 2048.
- [24] B. Zhang, Comput. Phys. Commun. 109 (1998) 193.
- [25] D. Molnar, M. Gyulassy, Nucl. Phys. A 698 (2002) 379.
- [26] J. Rak (for the PHENIX collaboration), nucl-ex/0306031.
- [27] B. Zhang, M. Gyulassy, Y. Pang, Phys. Rev. C 58 (1998) 1175.
- [28] Sen Cheng et al., Phys. Rev. C 65 (2002) 024901.
- [29] B. A. Li, A. T. Sustich, Phys. Rev. Lett. 82 (1999) 5004.
- [30] S.A. Voloshin, A.M. Poskanzer, Phys. Lett. B 474 (2000) 27.